Properties of amorphous semiconducting a-Si:H/a-SiN$_x$:H multilayer films and of a-SiN$_x$:H alloys

N. Ibaraki* and H. Fritzsche
James Franck Institute and Department of Physics, The University of Chicago, Chicago, Illinois 60637
(Received 25 June 1984)

We prepared, by plasma deposition and by alternating the plasma-gas mixture, multilayer films consisting of sequential layers of hydrogenated amorphous silicon (a-Si:H) of thickness d_1 and insulating amorphous silicon nitride (a-SiN$_x$:H) of thickness d_2. The thickness d_2 was held constant at 24 Å, while d_1 was changed from 12 to 2120 Å. Films with small d_1 had up to 180 layer pairs. The conduction and optical properties of these multilayer films were studied as well as the effect of prolonged light exposure (Staebler-Wronski effect). At large sublayer thickness $d_1 > 100$ Å the properties are dominated by space-charge doping which raises the Fermi level in the a-Si:H layers and leaves the nitride layers positively charged. At small sublayer thicknesses $d_1 < 50$ Å our observations are consistent with those of Abeles and Tiedje and their interpretation in terms of quantum-well confinement of charge carriers in the thin semiconductor sheets sandwiched between large-band-gap insulating layers. The properties of these multilayer films are compared with those of a-SiN$_x$:H alloys. These were prepared under the same plasma-decomposition conditions by changing the plasma-gas composition ratio of NH_3 to SiH_4 from 0.02 to 10.

I. INTRODUCTION

Multilayer structures or superlattices consisting of alternating layers of amorphous semiconductors should exhibit many of the interesting properties of crystalline semiconductor superlattices[1-3] except of course those that depend specifically on long carrier mean-free paths that do not exist in amorphous materials. However, amorphous multilayer structures have the advantage over single crystalline structures in that the materials need not be carefully selected so that the lattice constants of sequential layers are matched at their interfaces. The lack of this requirement for lattice matching allows the selection and combination of a large variety of amorphous materials, including semiconductors, insulators, and metals.

This work was motivated by our observations[4-6] that strong space charge layers are present in hydrogenated amorphous silicon (a-Si:H) whenever its surface is contacted with an insulator of different electronegativity such as an oxide layer, an adsorbate, or an insulating overlayer. These space charge layers usually dominate the electronic properties of high-quality a-Si:H films whose gap state density is less than about 5×10^{15} eV^{-1}cm^{-3}. One therefore expects large changes in the electrical and optical properties of an amorphous semiconductor when it is alternated in a multilayer structure with layers of an insulator that donates either electrons or holes and effectively shifts the Fermi energy in the semiconductor without the need of dopants.

We also noticed[7,8] that most of the current in a-Si:H field effect transistors is confined to a two-dimensional potential well whose dimension is 50 Å or less near the gate insulator. Under these conditions we predicted[8,9] that the extended state near the mobility edge of the amorphous semiconductor would become localized due to quantum confinement in the two-dimensional potential well and that the mobility edge would therefore shift to higher energies.

Studies of these two major effects, space-charge doping and quantum-well confinement, on the electrical and optical properties of a-Si:H have been started independently in several laboratories. Recently first results on such multilayer systems were reported by Munekata *et al.*,[10] Abeles *et al.*,[11,12] Tiedje *et al.*,[13] Kakalios *et al.*,[14] and Hirose and Miyazaki.[15] The properties of amorphous $As_{40}Se_{60}/Ge_{25}Se_{75}$ multilayer films have been reported by Ogino and Mizushima.[16] Work on multilayer amorphous thin-film structures has also been conducted at Energy Conversion Devices (ECD) during the last several years as reported in Ref. 14.

This paper describes in detail the optical and electrical properties of a-Si:H/a-SiN$_x$:H multilayers[14] having a-Si:H thicknesses between 12 and 2120 Å and a constant nitride thickness of about 24 Å. The properties of these multilayer films are compared with those of homogeneous alloys of a-SiN$_x$:H with x between $0 \le x \le 1.3$. These alloy films and the multilayer films were prepared under identical plasma-decomposition conditions.

II. EXPERIMENTAL DETAILS

The films were prepared in a capacitively coupled 13.65-MHz glow-discharge reactor. Six substrates were clamped onto each of the two capacitor plates that were heated to 250 °C. The plates had a diameter of 7 cm and were separated by 2.15 cm. A self-bias of about 80 V develops between the anode plate that is grounded to the stainless-steel chamber and the cathode plate that is connected to the rf power supply. For preparing the multilayered samples, the composition of the reactive gases was altered periodically between pure SiH_4 and a mixture having a composition ratio $r=[NH_3]/[SiH_4]=3.4$, while

the plasma was maintained continuously. The flow rate of SiH_4 was close to 29 cm^3/min at STP whereas that of NH_3 was about 100 cm^3/min at STP. The pressure in the plasma chamber was close to 0.1 Torr with pure SiH_4 and 0.25 Torr with the mixture of $r=3.4$. A liquid-nitrogen trap was located between the exit port and the rotary pump in order to increase the pumping speed of NH_3 and to achieve sharp compositional interfaces between layers. The rf power was chosen small enough so that the deposition rate was about 1.2 Å/s for anode samples. The deposition rate slowly increases with increasing r until $r=0.2$ and then drops to half its original value when r reaches 10.

For the series of multilayer samples the sublayer thickness d_1 of a-Si:H was varied from 12 to 2120 Å, while that of a-SiN_x:H was kept constant at 24 Å. The total thickness of the multilayer films were kept between 0.4 and 0.6 μm by varying the number M of sublayer pairs. The sublayer thicknesses were determined from the deposition rates of the individual sublayer materials. The values were in good agreement with the layer periods determined for $d_1 < 50$ Å from the positions of the first and second x-ray diffraction peaks.[14] In another series of samples, homogeneous films were grown from various gas mixtures $r=[NH_3]/[SiH_4]$ in the range $0 \le r \le 10$.

The electrical measurements were made along the film plane using either evaporated NiCr or painted graphite contacts having a length of 1.5 cm and a separation of approximately 0.2 cm. The layered films were scratched before applying the contacts in order to assure electrical contact to all layers. The current voltage curves were ohmic up to 250 V/cm, the highest field applied, in multilayer films with larger sublayer thickness, $d_1 > 500$ Å. A deviation from ohmicity at lower fields was observed for $d_1 < 200$ Å. All the data were taken in the ohmic region. Optical exposures were carried out with a heat-filtered tungsten-iodine lamp. The maximum light power at the sample was approximately $F_0 = 100$ mW/cm^2.

III. EXPERIMENTAL RESULTS: MULTILAYER FILMS

A. Optical properties

Figure 1 shows a Tauc plot of the optical-absorption coefficient α against photon energy $h\nu$ for layered samples with 12 Å $\le d_1 \le$ 47 Å as well as for pure a-Si:H and an alloy sample with $r=3.4$. This plot has the form

$$(\alpha h\nu)^{1/2} = B(h\nu - E_{\text{opt}}) , \tag{1}$$

where E_{opt} serves as a measure of the optical gap. The optical-absorption spectra of samples with $d_1 > 100$ Å were found to be indistinguishable from that of pure a-Si:H. One notices that the optical gap E_{opt} increases from 1.76 to 2.13 eV as d_1 is decreased from 50 to 12 Å. The slope B also increases noticeably in this range of the a-Si:H sublayer thickness d_1 in agreement with the measurements of Munekata *et al.*[10] This increase in the slope B is in sharp contrast to the gradual decrease in B that is observed, as shown later, when $[NH_3]/[SiH_4]$ is increased in alloy films. The homogeneous alloy film with $r=3.4$ has an optical gap of $E_{\text{opt}}=3.34$ eV and a slope $B=450$ (cm eV)$^{-1/2}$ which is considerably less than $B=870$ (cm eV)$^{-1/2}$ of pure a-Si:H.

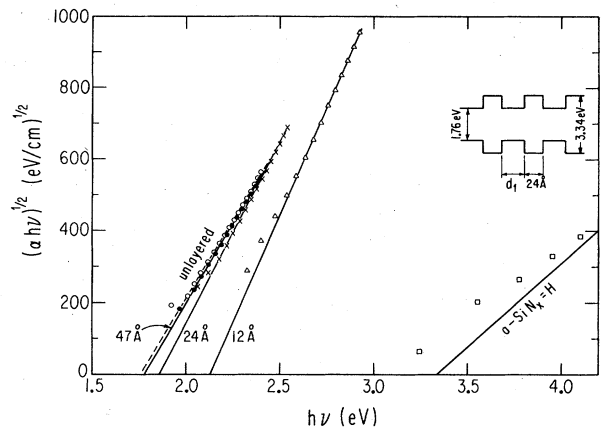

FIG. 1. Tauc plot of the optical absorption coefficient α in the form $(\alpha h\nu)^{1/2}$ against photon energy $h\nu$ for unlayered a-Si:H and a-SiN_x:H as well as for three multilayer films having an a-Si:H thickness $d_1 = 12$, 24, and 47 Å, respectively. The full line corresponding to unlayered a-SiN_x:H is determined by data points at higher values of $h\nu$.

At this point a brief note is appropriate that explains how we determined the absorption coefficient α. The transmittance and reflectance of multilayer structures can be obtained from the optical constants of the individual layers using the matrix method described by Ugur and Johanson.[17] In turn, the optical constants of a periodic repetition of two different materials can be deduced from the spectral dependence of the transmittance when the individual layer thicknesses are determined independently.

From the height and spacing of the interference fringes in the spectral dependence of the infrared transmittance we obtained the total film thickness d and an average dielectric constant ϵ. These are related to the thicknesses d_1, d_2 and dielectric constants ϵ_1, ϵ_2 of the individual layers by

$$\epsilon d = \epsilon_1 M d_1 + \epsilon_2 M d_2 , \tag{2}$$

where M is the number of sublayer pairs. Since the absorption of the a-SiN_x:H layers is negligible in the photon energy range $h\nu < 3.4$ eV the absorption leading to the α values of the multilayer films shown in Fig. 1 is solely due to the a-Si:H layers. In an alternative approach[11,13] one might treat the multilayer film as an average homogeneous medium of thickness d and a complex dielectric constant ϵ as expressed by Eq. (2). In that case the α values will be smaller by a factor $Md_1 n_1/dn$ and the values of B by a factor $(Md_1 n_1/dn)^{1/2}$, where n_1 and n are the refractive indices of a-Si:H and of the average medium, respectively.

The subband-gap absorption was measured with the photothermal deflection technique.[18] The results are shown in Fig. 2 for pure a-Si:H and for several multilayer films. The code (12,180) denotes a film with a-Si:H sublayers of thickness $d_1 = 12$ Å separated by $M=180$ nitride layers. The slope of the exponential Urbach edge of the absorption curve increases with decreasing d_1. A quanti-

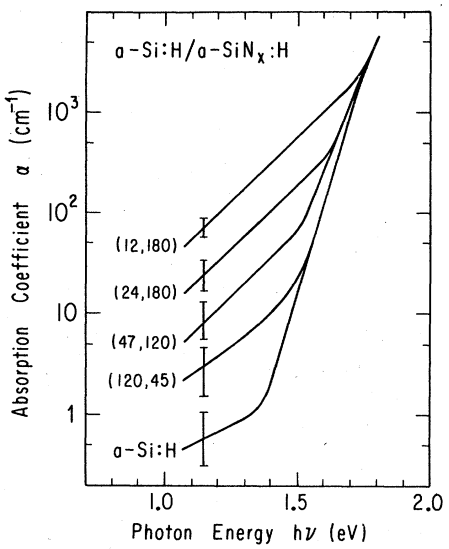

FIG. 2. Subband-gap absorption of a-Si:H and of multilayer films. The numbers in parentheses denote (d_1,M), the silicon sublayer thickness d_1 in angstroms and the number of double layers M. The vertical lines represent error bars of the low-absorption measurement and of smoothening the interference effects.

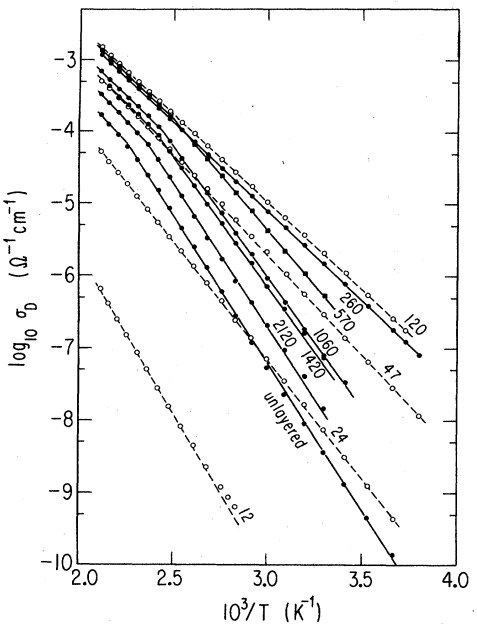

FIG. 3. Temperature dependence of the dark conductivity σ_D of unlayered a-Si:H and multilayer films after annealing in vacuum. The curves are labeled by the silicon sublayer thickness d_1 in units of Å.

tative determination of this change in slope was not possible because the increase of the low-energy absorption, that is attributed to gap and interface states, shortens the energy regime of the exponential Urbach tail too much to determine its slope with precision.

B. Dark conductivity

The dark conductivity σ_D was measured along the film plane after annealing each sample for 30 min at 200 °C in an oil-free vacuum of a molecular sieve pump (state A), as well as after exposure[19] to heat-filtered white light of $F_0=100$ mW/cm^2 for 60 min at 24 °C (state B). We used the sum of a-Si:H sublayer thicknesses $(M+1)\,d_1$ for converting the measured conductance into conductivity and thus neglected the very small conductance of the nitride insulators. Since we start and end the deposition with an a-Si:H layer, each film consists of $M+1$ silicon layers and M nitride layers.

Figure 3 shows that σ_D of state A follows:

$$\sigma_D=\sigma_0\exp(E_a/kT)\ . \tag{3}$$

Starting from pure unlayered a-Si:H, the conductivity first increases with decreasing d_1 and increasing number of layers. It reaches a maximum value for sample (120,45) and then decreases with decreasing d_1. Before the maximum is reached the conductivity curves show a kink toward a lower slope above 100 °C. This kink is absent in layered films having $d_1\leq 260$ Å. The conductivity prefactor σ_0 is plotted against the low-temperature activation energy E_a in Fig. 4. One finds that the samples fall into two groups, those having $d_1>260$ Å follow the Meyer-Neldel rule,[20]

$$\sigma_0=\sigma_{00}\exp(AE_a)\ , \tag{4}$$

with a slope $A=21$ eV^{-1} quite commonly observed in a-Si:H films,[9] whereas the multilayer films having $d_1<260$ Å have a prefactor σ_0 which is essentially constant and close to the theoretical value expected for the minimum metallic conductivity.[21] The strong dependence of σ_0 on E_a has been attributed to the shift of the Fermi energy E_F with temperature. This shift depends on the position of E_F and the energy dependence of the density of gap state near that energy.[22] It is interesting to note that this strong dependence disappears even for samples having $d_1>260$ Å if one restricts oneself to the conductivity measurements above the kink near 100 °C. This is shown by the crosses in Fig. 4 which represent the E_a and σ_0

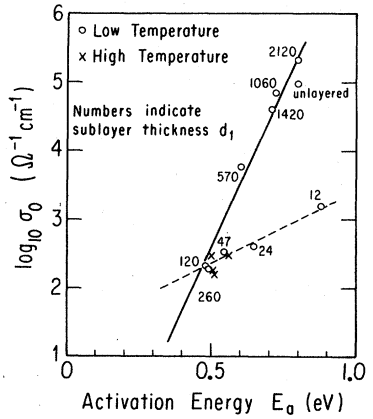

FIG. 4. Preexponential factor σ_0 as a function of conductivity activation energy E_a of annealed multilayer films having Si sublayer thickness d_1 as indicated. The crosses represent data points obtained for the unlayered and larger d_1 films at temperatures above the kink that occurs near 400 K in several of the conductivity curves shown in Fig. 3.

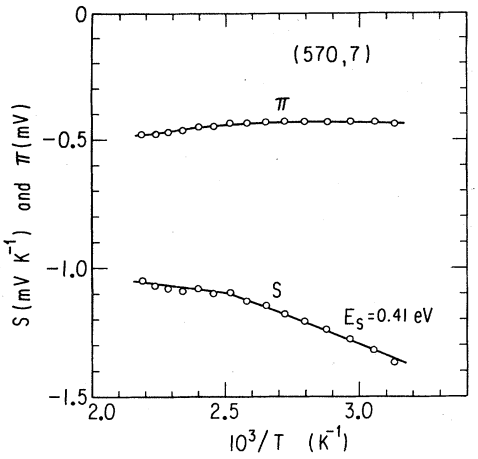

FIG. 5. The thermopower S and the Seebeck coefficient Π of a multilayer film having $d_1 = 570$ Å and $M = 7$.

data for the $d_1 > 260$ Å samples obtained from the high-temperature branch of the conductivity curves.

The kink is also observed in the temperature dependence of the thermopower S and the Peltier coefficient Π that are shown for sample (570,7) in Fig. 5. In agreement with earlier observations[23,24] on a-Si:H, the activation energy of the thermopower, 0.41 eV, is less than that of the conductivity, $E_a = 0.60$ eV, and the temperature dependence of the function $Q = \ln\sigma - (e/k)S$ does not exhibit the kink. The negative sign of the thermopower suggests that the nitride layers or their interfaces are positively charged. As d_1 becomes less than the screening length in a-Si:H the negative excess charge transferred from the nitride layers will be essentially uniformly distributed in the a-Si:H layers causing E_F to move upwards and E_a to decrease. Below $d_1 \simeq 50$ Å one enters a new regime in which spatial confinement of the carriers in quasi-two-dimensional quantum wells might become increasingly important.

Figure 6 summarizes the results discussed so far by showing the optical gap E_{opt}, the conductivity activation energy E_a, and the room-temperature dark conductivities $\sigma_D(A)$ and $\sigma_D(B)$ for pure a-Si:H and for layered films as a function of sublayer thickness d_1. For $d_1 > 40$ Å one observes a sizable Staebler-Wronski effect:[19] The dark conductivity after annealing, $\sigma_D(A)$, is considerably larger than that after light soaking with F_0 for 60 min, $\sigma_D(B)$. This effect essentially disappears for the layered samples with $d_1 < 40$ Å.

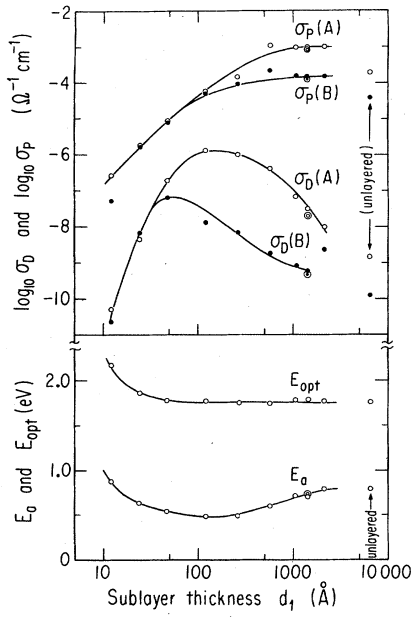

FIG. 6. Electronic parameters of multilayer films as a function of Si sublayer thickness d_1. At the right-hand side the data for an unlayered a-Si:H film are shown. E_a and E_{opt} are the conductivity activation energy and the optical gap, respectively. The dark conductivities σ_D and photoconductivities σ_P measured at room temperature are shown after annealing (A) and after prolonged light exposure (B).

C. Photoconductivity

The steady-state photoconductivity σ_P of state A and state B measured at room temperature with F_0 is also displayed in Fig. 6. The photoconductivity is increased about fivefold by introducing one insulating nitride layer (compare sample $d_1 = 2120$ Å with the unlayered film). The photoconductivity first remains fairly constant as d_1 decreases to $d_1 = 500$ Å. It begins to drop in a region where σ_D is still rising with decreasing d_1. It appears that at these small sublayer thicknesses recombination through interface states becomes increasingly dominant and the difference between states A and B disappears. The intensity dependence of the photoconductivity $\sigma_p \propto F^\gamma$ is governed by the exponent γ. This parameter changes with the introduction of the first insulating nitride film and again for sublayer thicknesses $d_1 < 500$ Å as is shown for states A and B in Fig. 7. The light intensity was kept below $10^{-2}F_0$ for measurements of state A.

Reporting photoconductivity parameters only at room temperature as we did in Figs. 6 and 7 is somewhat misleading as illustrated by the examples shown in Figs. 8 and 9. These figures show the temperature dependence of σ_D and σ_P in states A and B of a layered film (120,45) and an unlayered a-Si:H film, respectively. The data were

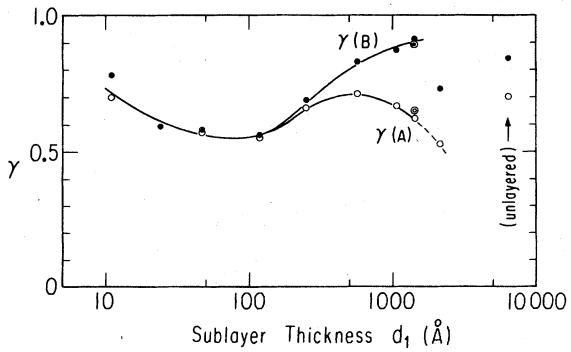

FIG. 7. Exponent γ that determines the dependence of σ_P on light intensity after annealing (A) and after prolonged light exposure (B). The circled data points correspond to a multilayer sample that was prepared with special care to prevent nitrogen contamination of the silicon layer.

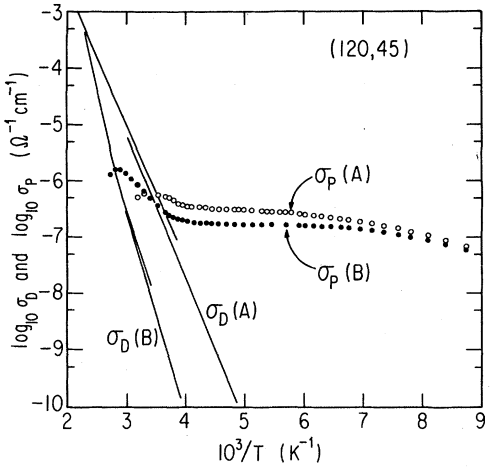

FIG. 8. Temperature dependence of the dark conductivity σ_D and photoconductivity σ_P of a multilayer film ($d_1=120$ Å, $M=45$) after annealing (A) and after light exposure (B).

taken with $F=10^{-3}F_0$ in order not to induce defect states by light. There is still a noticeable difference between σ_P(A) and σ_P(B) of the sample with $d_1=120$ Å except by chance near room temperature, for which the values are plotted in Fig. 6.

The photoconductivity is nearly independent of temperature below $T=250$ K. Normally one finds that σ_P increases with T because with increasing T the quasitrap Fermi levels move away from their respective mobility edges, thereby reducing the number of recombination centers that are bracketed between these quasitrap Fermi levels. A reduction in the number of recombination centers in turn results in an increase in free-carrier lifetime and hence an increase of the photoconductivity with temperature. A constant σ_P therefore means that the number of recombination centers is constant which implies that these centers are located not too far from the gap center. In other words, the main recombination traffic appears to pass through deep gap states and not through the localized band-tail states. If these deep gap states give rise to the subband-gap absorption that is shown in Fig. 2, then their increase with decreasing sublayer thickness d_1 might explain the observed decrease in σ_P. The details of the recombination processes need further study because the interfaces are likely to play an important role.

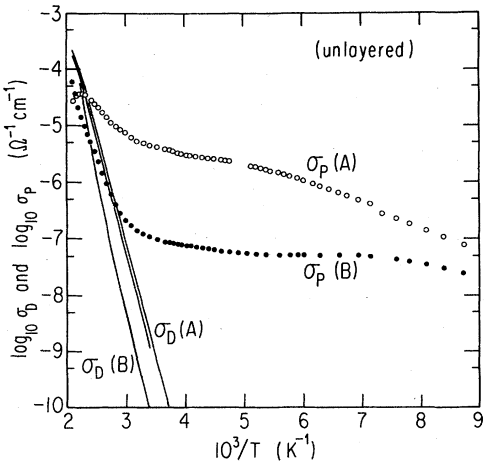

FIG. 9. Temperature dependence of the dark conductivity σ_D and the photoconductivity σ_P of an unlayered a-Si:H film after annealing (A) and after prolonged light exposure (B).

IV. EXPERIMENTAL RESULTS: a-SiN$_x$:H ALLOYS

One of the crucial questions in interpreting the properties of the multilayer films concerns the sharpness of the concentration gradient at the interfaces. This is related to the question of how much of the NH_3 remains in the plasma chamber while the next a-Si:H sublayer is growing and how much the properties of the multilayer structures are affected by some nitrogen alloying. We tried to answer this question by studying the effect of nitrogen on the electrical and optical properties of a-SiN$_x$:H alloy films that were prepared under practically the same plasma conditions as the multilayer films.

Figure 10 shows the optical gap $E_{\rm opt}$, the conductivity activation energy E_a of state A, the dark conductivities σ_D(A), σ_D(B) as well as the photoconductivities $\sigma_P(A)$ and $\sigma_P(B)$ of states A and B, respectively, of pure a-Si:H and of the silicon-nitride alloys as a function of the plasma-gas ratio $r=[NH_3]/[SiH_4]$. These are room-temperature values and σ_P was measured with the heat-filtered light flux F_0. The gas ratio $r=3.4$ used for the insulating layers in the layered structures is marked by a vertical arrow in Fig. 10. At this alloy concentration the material is highly insulating with an optical gap of

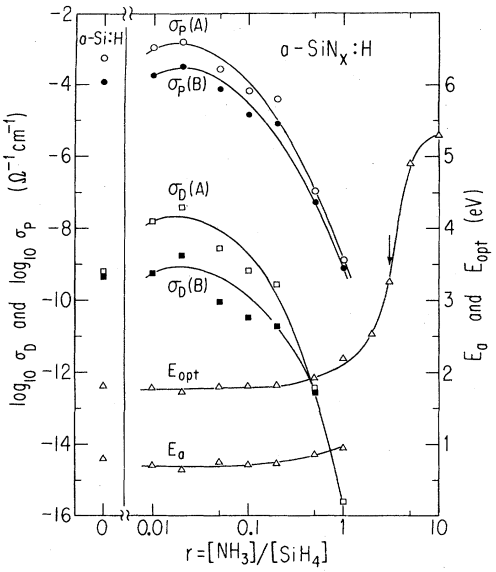

FIG. 10. Electronic parameters of a-SiN$_x$:H alloy films as a function of plasma gas ratio $r=[NH_3]/[SiH_4]$. E_a and $E_{\rm opt}$ are the conductivity activation energy and the optical gap, respectively. The dark conductivities σ_D and photoconductivities σ_P measured at room temperature are shown after annealing (A) and after prolonged light exposure (B).

$E_{opt}=3.34$ eV and a conductivity of less than 10^{-16} $\Omega^{-1}\,cm^{-1}$ as determined from the leakage current measured normal to the film plane.

We wish to point out the following main features of the results shown in Fig. 10. Both σ_D and σ_P reach a maximum near $r=0.02$ and then decrease quite rapidly with increasing r. A large Staebler-Wronski effect[19] is observed up to gas ratios of $r=0.2$. The optical gap E_{opt} as well as the conductivity activation energy E_a hardly change up to $r=0.2$; above that value they increase with increasing r. The rapid decrease of σ_D while E_a remains nearly constant between $r=0.02$ and 0.2 shows that a-SiN_x:H alloy films do not follow the Meyer-Neldel rule. The preexponential factor σ_0 actually decreases with increasing r and hence with increasing E_a; it is $\sigma_0=10$ $(\Omega\,cm)^{-1}$ at $r=1.0$ where $E_a=0.95$ eV. This unusually low value of σ_0 at such a large activation energy suggests that the a-SiN_x:H is not homogeneous but consists of silicon-nitride particles which constrict the conducting percolation path through regions which contain less nitrogen.[25] Unlike other group-V elements nitrogen does not act as a donor in crystalline silicon[26] because of its small size and its large-sp^3 promotion energy. The slight increase in σ_D and the decrease in E_a noticeable in Fig. 10 between $r=0$ and 0.02 might be a doping effect but it may also be due to a charge transfer from positively charged nitride particles to surrounding a-Si:H.

In contrast to the large change in photoconductivity the exponent γ, which governs the dependence of σ_P on the incident light flux F, remains nearly constant as the plasma-gas ratio is changed from zero to $r=1.0$. This is shown for states A and B at room temperature in Fig. 11. The constancy of γ suggests that the recombination process is not greatly affected by the large nitrogen content even though the recombination lifetime is shortened by five orders of magnitude between $r=0.2$ and 1.

Even though the optical gap E_{opt} remains nearly unchanged up to $r=0.2$, both the slope B of the Tauc plot [Eq. (1)] and the refractive index n measured near $\lambda=2$ μm decrease as soon as NH_3 is added to the plasma gas. These parameters are shown as a function of r in Fig. 12. This trend is not inconsistent with a heterogeneous model for the a-SiN_x:H alloys containing nitride-rich particles. Still more work is required before these questions can be answered more definitively.

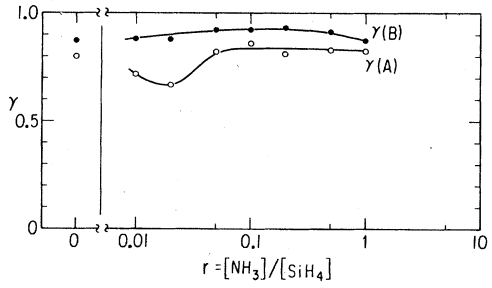

FIG. 11. The exponent γ that governs the power-law dependence of σ_P on light intensity as a function of plasma-gas ratio after annealing (A) and after prolonged light exposure (B).

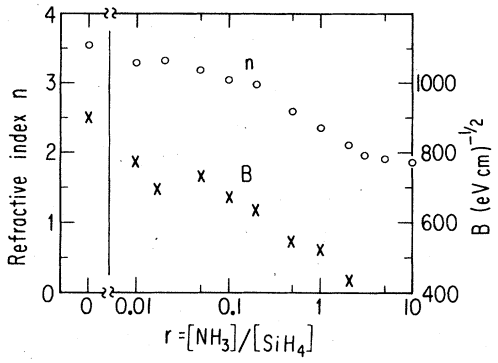

FIG. 12. The refractive index n measured near $\lambda=2$ μm and the slope B of the Tauc plot of optical absorption [see Eq. (1) of text] as a function of plasma-gas ratio r for a-SiN_x:H alloy films.

V. DISCUSSION

A. Concentration gradients

The properties of our a-Si:H/a-SiN_x:H multilayer films agree closely with those reported by Abeles *et al.*[11,12] who prepared their films in a similar manner in one reaction chamber by switching on and off the NH_3 supply to the plasma reactor while maintaining the silane flow and the plasma. We presented here in addition a detailed study of the a-SiN_x:H alloy system in order to shed some light on the question of whether the anomalous properties of thin multilayer structures are caused by quantum-well effects or by alloying of the a-Si:H layers with residual nitrogen. Some alloying must take place because even if 99% of the NH_3 used for the growth of the nitride layers is swept out faster than the 1.0 s needed to grow a monolayer of a-Si:H the remaining amount of $r=0.01$ does not cause significant changes in the properties of the alloy films. The presence of a second-order x-ray diffraction peak observed[14] in the three films having the shortest superlattice period indicates that the concentration profile varies faster than sinusoidally. This, however, does not rule out the presence of a few atomic percent nitrogen in the a-Si:H layers. On the contrary, considering the dwell times of NH_3 in plasma systems,[27] it is likely that the silicon layers contain a certain amount of nitrogen which we estimate to be a few percent. Furthermore, the nitrogen-concentration gradient will likely be less steep when a-Si:H grows on the nitride layer after switching off the NH_3 supply than at the interface formed when the NH_3 is switched on.

In order to check whether a concentration gradient at one of the pairs of interfaces had an undue effect on the transport properties, we prepared one multilayer film, having three sublayers of a-Si:H with $d_1=1420$ Å and two layers of 24 Å SiN_x:H, by pumping and flushing the plasma gas for 15 min after each silicon nitride deposition. This procedure also required extinguishing the plasma for that length of time. The results of the measurements on that sample are marked with the circled data points in Fig. 6. There is essentially no difference between this sample and the one prepared by switching the NH_3

supply on and off without extinguishing the plasma. From this we conclude that even though the interfaces are probably not atomically sharp but exhibit a gradient in the nitrogen concentration, this gradient does not give rise to the major effects observed in the multilayer films. These effects are discussed in the following by considering the regimes of small and of large sublayer thicknesses separately.

B. Small sublayer thicknesses

As shown in Fig. 6 the optical and electrical properties change when the a-Si:H sublayer thickness d_1 becomes less than 50 Å. The rise of the optical gap and the rise of the conductivity activation energy are nearly parallel. This agrees qualitatively with the findings of Abeles and Tiedje[11] and Tiedje *et al.*[13] The latter authors calculate an average absorption coefficient α of the total film. We calculate α for the a-Si:H layers using Eq. (2). An increase in $E_{\rm opt}$ and E_a is consistent with a rise of the mobility edge due to localization of states near the mobility edge on account of the confinement of electrons (and holes) in the one-dimensional potential well formed by the a-Si:H sublayers between the wide-band-gap nitride layers. We cannot explain the increase of the slope B with decreasing d_1 but this behavior is opposite to the effect of adding nitrogen to a-Si:H that decreases the slope B as shown in Fig. 12. This increase of B for the smallest sublayer thicknesses d_1 may therefore be related to the potential-well effect.

We wish to emphasize at this point that the analysis of Ugur and Johanson[17] assumes that the layers are perfectly uniform and parallel and that the interfaces are abrupt. Amorphous silicon layers that are 12—24 Å thick must have a considerable roughness if the deposition occurs statistically without a lateral smoothening process. In addition there will be the concentration gradient at the interfaces due to the finite residence and mixing times at the changes of gas composition in the plasma chamber. Abeles *et al.*[12] presented evidence that the layers in their multilayer films are indeed much smoother than would be expected from a statistical model. We do not have similar proof of the quality of our films and thus have to allow for the possibility that the thickness dependence of the constant B of the Tauc plot results from assuming greater smoothness and uniformity than exists in our films.

The increase in conductivity activation energy E_a with decreasing d_1 does not result in the usual increase in the prefactor σ_0 as shown in Fig. 4. If the temperature shift of the Fermi level is the major cause of the Meyer-Neldel increase of σ_0 with E_a in normal samples, as claimed,[22] then we conclude that a fairly constant density of interface states essentially pins the Fermi level in thin multilayer films and thus gives rise to a σ_0 value close to that of the expected minimum metallic conductivity. These interface states may also be the cause for the rise in subband-gap absorption shown in Fig. 2 and the decrease in σ_P with decreasing d_1.

The agreement of σ_0 of our film having $d_1=12$ Å with the value predicted for three-dimensional conduction near a mobility edge means that we find no evidence for the theoretical prediction[28] that extended states cease to exist in two-dimensional disordered systems. This is not too surprising because our sample hardly qualifies as a test of the theory because of the high measuring temperature and the nonideality of its quasi-two-dimensional structure.

At small values of d_1 there is no Staebler-Wronski effect observed in terms of light-induced changes in σ_D or σ_P. This is to be expected when the Fermi level is fairly well pinned by interface states. Nevertheless, light still creates metastable defect states even in the thinnest d_1 multilayer films: Regardless of the value of d_1 we observed[14] a photoluminescence fatigue of about $8\pm2\%$ after exposure at 78 K to an exposure to 5×10^{21}-cm^{-2} photons of $h\nu=2.4$ eV.

C. Large sublayer thicknesses

Between $d_1=2000$ and 100 Å the dark conductivity σ_D rises and its activation energy E_a decreases from 0.8 to 0.48 eV with decreasing d_1. We believe that this is the result of space-charge doping, i.e., a transfer of electrons from the nitride layers and/or their interfaces to the a-Si:H layers. In order to understand the functional dependence of σ_D or of E_a on d_1 one must consider the fact that d_1 becomes small compared to the space-charge width. This problem has been treated by Redfield[29] and Powell and Pritchard.[30] The layered sample with $d_1=2120$ Å contains only one nitride layer in its center. Its small changes in σ_D and E_a compared to the values of the unlayered film indicate that only a small band bending of about 0.03—0.04 eV and a correspondingly small charge transfer occurred. The fact that σ_D increases and E_a continues to decrease as d_1 is reduced may be understood qualitatively as follows. Since d_1 is less than the screening length, the total negative charge transferred to the a-Si:H layer must move the Fermi energy further up as d_1 decreases. The limiting value will be given by the energy position of the donor states associated with the nitride layer. A quantitative analysis is not possible at present because of the dependence of σ_0 on E_a in this regime shown in Fig. 4.

The increase in photoconductivity by a factor of 5 between the unlayered and the first-layered films is not large enough to single out one of several explanations. This increase should be contrasted, however, with a decrease in σ_P by about three orders of magnitude that is often observed when the thickness of an ordinary, undoped a-Si:H film is reduced from say 1.2 μm to 1400 Å.[31] This reduction is normally attributed to surface recombination. The fact that σ_P of the layered films remains higher than that of an unlayered film down to $d_1=120$ Å is therefore remarkable. It may be associated with an internal field[32] in the sublayers that induces a spatial separation of the trapped photocarriers and hence a reduction in the recombination rate.

The persistence of the Staebler-Wronski effect of multilayer films to the smallest sublayer thickness $d_1=12$ Å (based on the observation of fatigue of the photoluminescence) and in a-SiN_x:H alloys to considerable nitrogen concentrations suggests that the number of photocreated defect states does not become swamped by a very large

density of defects already present in the multilayer and alloy films. Yet, the subband-gap absorption (see Fig. 2) of the thinnest multilayer films is much higher than that produced by prolonged light exposure of unlayered films.[33] This suggests that the defects giving rise to the subband-gap absorption are spatially separated from the regions in which photoluminescence and its fatigue are taking place. Perhaps one can still distinguish a defect-rich interface region and a relatively high-quality a-Si:H region even in $d_1=12$- and 24-Å films. This view is further supported by the observation[14] that the photoluminescence intensity of the thinnest multilayer films (12,180) is only a factor of 6 less at 78 K than that of the unlayered film even though the absorption near $h\nu=1$ eV and therefore the density of deep states is larger by a factor of 100.

VI. SUMMARY AND CONCLUSIONS

Our studies of amorphous semiconductor multilayers consisting of alternating layers of undoped a-Si:H and insulating a-SiN_x:H show two distinct regimes. At a-Si:H sublayer thickness $d_1 > 100$ Å we observe space-charge doping which raises the Fermi energy by about 0.4 eV. The nitride layers become positively charged. The photoconductivity is increased relative to an unlayered film despite a probably increased recombination through interface states. When the a-Si:H sublayer thickness becomes less than $d_1 < 50$ Å we observe, in agreement with Abeles and Tiedje[11] and Ogino and Mizushima,[16] a widening of the optical gap and an increase of the conductivity activation energy. This effect is consistent with localization of states near the mobility edge as a result of the one-dimensional confinement of electrons and holes in the potential wells formed by the thin a-Si:H layers sandwiched between the wide-band-gap nitride layers.

A comparison of the multilayer structures with a-SiN_x:H alloy containing different concentrations of nitrogen indicates that the main properties of the multilayer films are governed by charge-exchange doping of electrons from the nitride to the silicon layers as well as by quantum-well effects. We cannot exclude the possibility that the nitrogen concentration at the interfaces is graded and that a few atomic percent of nitrogen are incorporated in the a-Si:H layers.

A fatigue of the photoluminescence of about $8\pm2\%$ after light exposure to 5×10^{21} cm^{-2} photons at 78 K is observed[14] in all multilayer films independent of the a-Si:H sublayer thickness d_1. The rate of fatigue as well as its annealing behavior suggests that it is a consequence of light-induced defect creation as the Staebler-Wronski effect.[19] If this interpretation is correct then the persistence of the fatigue down to $d_1=12$ Å implies that the background of defects is not raised much by decreasing the sublayer thickness d_1. Yet, the increase subband-gap absorption and the constancy of the conductivity prefactor σ_0 with decreasing d_1 suggests the presence of interface defects near the gap center.

Measurements of thermostimulated currents and of the drift mobility[34] in these multilayer films by means of the traveling-wave method as well as a study of doping-modulated a-Si:H (Ref. 35) have been undertaken and will be reported elsewhere.

ACKNOWLEDGMENTS

We wish to thank J. Kakalios and H. Ugur for initial help and guidance in preparing and characterizing the samples and many fruitful discussions. We are grateful to S. Payson of Energy Conversion Devices for carrying out the low-absorption measurements by means of the photothermal deflection method. The work was supported in part by Energy Conversion Devices and the National Science Foundation (NSF), Grant No. DMR8009225. One of us (N.I.) would like to thank the Toshiba Corporation for financial support and for partial support of this research. The materials were prepared in the Material Research Laboratory of the University of Chicago supported by NSF.

*Present address: Toshiba Electron Device Engineering Laboratory, 8 Shinsugita-cho, Isogo-Ku, Yokohama, 235 Japan.

[1]L. Esaki and R. Tsu, IBM J. Res. Dev. **14**, 61 (1970).
[2]R. Dingle, in *Festkörperprobleme Advances in Solid State Physics*, edited by H. J. Queisser (Pergamon, New York, 1975), Vol. XV, pp. 21–49.
[3]C. H. Döhler, Sci. Am. **249**(5), 144 (1983), and references therein.
[4]M. Tanielian, H. Fritzsche, C. C. Tsai, and E. Symbalisty, Appl. Phys. Lett. **33**, 353 (1978).
[5]M. Tanielian, M. Chatani, H. Fritzsche, V. Smid, and P. D. Persans, J. Non-Cryst. Solids **35&36**, 575 (1980).
[6]B. Aker and H. Fritzsche, J. Appl. Phys. **54**, 6628 (1983).
[7]Nancy B. Goodman and H. Fritzsche, Philos. Mag. B **42**, 149 (1980).
[8]H. Fritzsche, Sol. Cells **2**, 289 (1980).
[9]H. Fritzsche, Sol. Energy Mater. **3**, 447 (1980).
[10]H. Munekata, M. Mizuta, and H. Kukimoto, J. Non-Cryst. Solids **59&60**, 1167 (1983); H. Munekata and H. Kukimoto, Jpn. J. Appl. Phys. **22**, L544 (1983).
[11]B. Abeles and T. Tiedje, Phys. Rev. Lett. **51**, 2003 (1983).
[12]B. Abeles, T. Tiedje, K. S. Liang, H. W. Deckman, H. C. Stasiewski, J. C. Scanlon, and P. M. Eisenberger, J. Non-Cryst. Solids **66**, 351 (1984).
[13]T. Tiedje, B. Abeles, P. D. Persans, B. G. Brooks, and G. D. Cody, J. Non-Cryst. Solids **66**, 345 (1984).
[14]J. Kakalios, H. Fritzsche, N. Ibaraki, and S. R. Ovshinsky, J. Non-Cryst. Solids **66**, 339 (1984).
[15]M. Hirose and S. Miyazaki, J. Non-Cryst. Solids **66**, 327 (1984).
[16]T. Ogino and Y. Mizushima, Jpn. J. Appl. Phys. **22**, 1647 (1983).
[17]H. Ugur and R. Johanson (unpublished).
[18]W. B. Jackson, N. M. Amer, A. C. Boccara, and D. Fournier, Appl. Opt. **20**, 1333 (1981).
[19]D. L. Staebler and C. R. Wronski, Appl. Phys. Lett. **31**, 292

(1977); J. Appl. Phys. **51**, 3262 (1980).
[20]W. Meyer and H. Neldel, Z. Tech. Phys. **18**, 588 (1937).
[21]N. F. Mott and E. A. Davis, in *Electronic Processes in Non-Crystalline Materials* (Clarendon, Oxford, 1979).
[22]H. Overhof and W. Beyer, Phys. Status Solidi B **107**, 207 (1981).
[23]W. Beyer and H. Overhof, Solid State Commun. **31**, 1 (1979).
[24]H. Overhof and W. Beyer, Philos. Mag. B **43**, 433 (1981).
[25]H. R. Philipp, J. Electrochem. Soc. Jpn. **120**, 295 (1973); S. C. H. Lin and M. Joshi, *ibid.* **116**, 1740 (1969).
[26]J. B. Mitchell, J. Shewchun, T. A. Thomson, and J. A. Davies, J. Appl. Phys. **46**, 335 (1975); W. Kaiser and C. D. Thurmond, *ibid.* **30**, 427 (1959).
[27]C. C. Tsai (private communication); see also C. C. Tsai, J. C. Knights, R. A. Lujan, B. Wacker, B. L. Stafford, and M. J. Thompson, J. Non-Cryst. Solids **59& 60**, 731 (1983).
[28]E. Abrahams, P. W. Anderson, D. C. Licciardello, and R. V. Ramakrishnan, Phys. Rev. Lett. **42**, 673 (1983).
[29]D. Redfield, J. Appl. Phys. **54**, 2860 (1983).
[30]M. J. Powell and J. Pritchard, J. Appl. Phys. **54**, 3244 (1983).
[31]H. Fritzsche, in *Semiconductors and Semimetals,* edited by J. I. Pankove (Academic, New York, 1984), Vol. 21, Part C.
[32]C. B. Roxlo, B. Abeles, and T. Tiedje, Phys. Rev. Lett. **52**, 1994 (1984).
[33]N. M. Amer and W. B. Jackson, in *Semiconductors and Semimetals,* Ref. 31, Part B.
[34]H. Ugur and H. Fritzsche, Solid State Commun. (to be published).
[35]J. Kakalios, H. Fritzsche, and K. L. Narasimhan, Proceedings of the International Conference on Optical Effects in Amorphous Semiconductors, Snowbird, Utah (AIP, New York, in press); J. Kakalios and H. Fritzsche, Proceedings of the International Conference on the Physics of Semiconductors, San Francisco, California, 1984 (Springer, New York, in press).